Nonlinear static analysis of smart beams under transverse loads and thermal-electrical environments

Hayder A.K. Ali[2], Mouayed H.Z. Al-Toki[*1], Raad M. Fenjan[2], Nadhim M. Faleh[2]

[1]*Middle Technical University, Technical College, Baghdad, Iraq*
[2]*Al-Mustansiriah University, Engineering Collage P.O. Box 46049, Bab-Muadum, Baghdad 10001, Iraq*

Abstract. This research has been devoted to examine nonlinear static bending analysis of smart beams with nano dimension exposed to thermal environment. The beam elastic properties are corresponding to piezo-magnetic material of different compositions. The large deflection analysis of the beam has been performed assuming that the beam is exposed to transverse uniform pressure. Based on the rule of Hamilton, the governing equations have been derived for a nonlocal thin beam and solved using differential quadrature method. Temperature variation effect on nonlinear deflection of the smart beams has been studied. Also, the beam deflection is shown to be affected by electric voltage, magnetic intensity and material composition.

Keywords: beam theory; bending; nonlocal theory; numerical analysis; static behavior; thermal load

1. Introduction

Novel materials under multi-physical fields have extraordinary behavior, especcialy when the fields are coupled to each other. As an instance, MEE materials display mechanical deformation under magnetic or electric field (Singh and Kumari 2020, Pan and Han 2005). The above fact is associated with the coupling of magnetic-electric and elastic fields (Li and Shi 2009, Guo *et al*. 2016). In such materials, the material charactrics may be especified from elastic, piezoelectric and magnetic components. Structural components (beams, shells and plates) made of MEE materials have been commonly exploited for actuating and sensing in smart machines. The material distribution in these structures may be homogenous or non-homogenous. By assuming the varying material profiles within the thickness of structures, the material distributions have been considered to be nonhomogenous. As an example, a functional graded material is a non-homogenous material in which two materials are involved and all material properties change from one material to another. In regard to the percentages and volume fractions of each material, the effective properties of the structures may be charactrized. There are several investigations on smart piezoelectric-magnetic-elastic structures having functionally graded distribution (Kumaravel *et al*. 2007).

---

*Corresponding author, Ph.D., E-mail: mouayedaltoki@mtu.edu.edu.iq

Many expriments and investigations have been carried out on various materials and structures (Jiang *et al*. 2021, Zhou *et al*. 2021). According to recent analysis and nano-scale simulations, it has been stated that the mechanical attributes of nano-sized piezo-electric and piezo-magnetic structures are relied on small scale effects (Ahmed *et al*. 2019, Al-Maliki *et al*. 2019, Fenjan *et al*. 2019). However, owning to the reason that classical continuum modelling has been identified as a scale-independent approach, studying and exploring the mechanical specifications of a low-dimension structure via classical continuum mechanics gives fallacious results and subsequently incorrect designing. Albeit, the atomistic modelling and molecular simulation are affective approaches for establishing the scale-dependent specifications of low-dimension structures, their utilization is not more reasonable owning to the need for numerous computational efforts. For reducing the computational efforts, a number of scale-dependent mechanical models which include the nonlocal elasticity theory (Eringen 1972), strains gradient elasticity theory, refined couple stresses theory and etc, have been developed for accommodating low-dimension factors by introducing the scale parameters and have been widely employed for studying the mechanical specifications of micro or nano structures (Thai and Vo 2012, Akbas 2016, Abdullah *et al*. 2021, Ahmed *et al*. 2020, 2021, Raheef *et al*. 2021, Fenjan *et al*. 2020a, b, Abdulrazzaq *et al*. 2020, Al-Maliki *et al*. 2020, Hamad *et al*. 2019, Muhammad *et al*. 2019). The intelligent materials introduced in the prior paragraphs have been widely exploited in nano-structures and nano-devices (Ke *et al*. 2014, Liu *et al*. 2018). Furthermore, at the nanoscale, the behaviors of structures are different from macro scale structures. Such behaviors are owning to the inclusion of low-dimension influences. The low-dimension influences have been included in higher-order elasticity theories, for example Eringen's elasticity, which is also applied by other researchers.

Analysis of nonlinear bending behaviors of composite magneto-electro-elastic (MEE) nano-scale beams have been represented in this reaserch. The beam is assumed to be under a transverse mechanical load. Composite MEE material has been produced form piezoelectric and magnetic ingradients in which the material charactristics may be varied according to the percentages of the ingradients. The governing equations including scale effects have been developed in the framework of nonlocal elasticity. It has been demonstrated that nonlinear bending behaviors of MEE nano-sized beams in electrical-magnetic fields rely on the percentages of the ingradients. Also, the efficacy of nonlocality parameter, magnetic intensities and electrical voltages on stability loads of the nanobeams have been researched.

2. Theory of non-local elasticity for piezo-magnetic structures

According to the theory of non-local elasticity for smart magnetic-piezoelectric-elastic materials, stresses σ_{ij} electrical displacements D_i and magnetic inductions B_i can be defined in below form:

$$\sigma_{ij} = \int_V \alpha\big(|x' - x|, \tau\big)\, [C_{ijkl}\varepsilon_{kl}(x') - e_{mij}E_m(x') - q_{nij}H_n(x')]dV(x') \tag{1a}$$

$$D_i = \int_V \alpha\big(|x' - x|, \tau\big)\, [e_{ikl}\varepsilon_{kl}(x') + s_{im}E_m(x') + d_{in}H_n(x')]dV(x') \tag{1b}$$

$$B_i = \int_V \alpha\big(|x' - x|, \tau\big)\, [q_{ikl}\varepsilon_{kl}(x') + d_{im}E_m(x') + \chi_{in}H_n(x')]dV(x') \tag{1c}$$

where V defines the volume. Above relations are associated with strains ε_{kl}, and electric-

magnetic field (E_m, H_n). Till to now, mechanical analysis of piezo-magnetic nano-structures is performed based on diverse values for nonlocal parameter. Some of papers used actual value of nonlocal parameter with unit of *nm*, but some papers used normalized values for nonlocal factor in such a way that nonlocal parameter is normalized with respect to the length of nano-structure. Ke *et al*. (2014) and other authors used normalized values for nonlocal parameter as μ = e₀a/ L = 0.1~0.3 for studying vibrations of smart nanobeams with length *L*. Also, all components of stress field, electrical field displacement (D_i) and magnetic induction (B_i) for a scale-dependent shell associated with nonlocal elasticity may be introduced by:

$$\sigma_{ij} - (e_0 a)^2 \nabla^2 \sigma_{ij} = C_{ijkl} \varepsilon_{kl} - e_{mij} E_m - q_{nij} H_n \tag{2a}$$

$$D_i - (e_0 a)^2 \nabla^2 D_i = e_{ikl} \varepsilon_{kl} + s_{im} E_m + d_{in} H_n \tag{2b}$$

$$B_i - (e_0 a)^2 \nabla^2 B_i = q_{ikl} \varepsilon_{kl} + d_{im} E_m + \chi_{in} H_n \tag{2c}$$

3. MEE composites

A nanobeam of dimension *L* and *h* has been shown in Fig. 1. This nanobeam is made of a MEE composite having two phases: a piezoelectric phase $BaTiO_3$ with volume fraction V_f and a magnetic phase $CoFe_2O_4$. All of material properties for the phases can be found in Table 1 which contains elastic (C_{ij}), piezo-electrical (e_{ij}) and magnetics (q_{ij}) coefficients. Furthermore, k_{ij}, d_{ij} and x_{ij} respectively express the coefficients of dielectrics, magnetic-electrical and magnetic permeabilities.

Table 1 Material properties for piezo-magnetic beam made of $BaTiO_3$-$CoFe_2O_4$

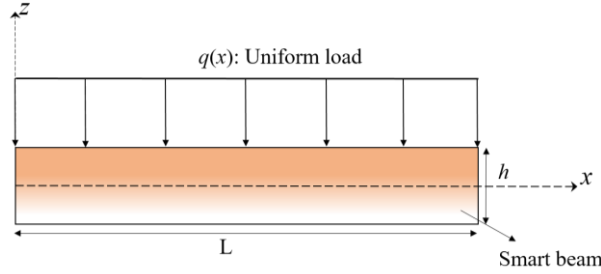| Property	V_f= 0%	20%	40%	60%	80%
C_{11} (*GPa*)	286	250	225	200	175
C_{13}	170	145	125	110	100
C_{33}	269.5	240	220	190	170
e_{31} (*C/m²*)	0	-2	-3	-3.5	-4
e_{33}	0	4	7	11	14
q_{31} (*N/Am*)	580	410	300	200	100
q_{33}	700	550	380	260	120
k_{11} (*10⁻⁹ C/Vm*)	0.08	0.33	0.8	0.9	1
k_{33}	0.093	2.5	5	7.5	10
d_{11} (*10⁻¹² Ns/VC*)	0	2.8	4.8	6	6.8
d_{33}	0	2000	2750	2500	1500
x_{11} (*10⁻⁴ Ns²/C²*)	-5.9	-3.9	-2.5	-1.5	-0.8
x_{33}	1.57	1.33	1	0.75	0.5
α_1 (*10⁻⁶*)	10	11.7	13	14.11	14.98
α_3	10	9.72	9.15	8.37	7.44

Fig. 1 A mechanically loaded beam

4. Beam formulation

There are different theories for modeling of beam and plate structural components (Polatov *et al.* 2020, Heydari 2020, Abderezak *et al.* 2021). By using thin beam theory for a smart nanobeam, the displacement field which contains longitudinal (u), (w) components can be expressed as follows:

$$u_1(x,z) = u(x) - z\frac{\partial w}{\partial x}(x) \tag{3}$$

$$u_3(x,z) = w(x) \tag{4}$$

Above field components result in below relations for the strain field:

$$\varepsilon_{xx} = \frac{\partial u}{\partial x} - z\frac{\partial^2 w}{\partial x^2} + \frac{1}{2}\left(\frac{\partial w}{\partial x}\right)^2 \tag{5}$$

The induced electro-magnetic field having electric potential (Φ) and magnetic potential (Υ) to the nano-scale beam can be expressed as:

$$\Phi(x,z) = -cos(\xi z)\phi(x) + \frac{2z}{h}V_E \tag{6}$$

$$\Upsilon(x,z) = -cos(\xi z)\gamma(x) + \frac{2z}{h}\Omega \tag{7}$$

with $\xi = \pi/h$. Next, V_E and Ω define the exterior electrical voltages and magnetic potentials induced to the smart beam. All ingredients of electrical field (E_x, 0, E_z) and magnet field (H_x, 0, H_z) can be obtained as:

$$E_x = -\Phi_{,x} = cos(\xi z)\frac{\partial \phi}{\partial x}, \tag{8}$$

$$E_z = -\Phi_{,z} = -\xi \, sin(\xi z)\phi - \frac{2V}{h} \tag{9}$$

$$H_x = -\Upsilon_{,x} = cos(\xi z)\frac{\partial \gamma}{\partial x}, \tag{10}$$

$$H_z = -Y_{,z} = -\xi \sin(\xi z)\gamma - \frac{2\Omega}{h} \qquad (11)$$

Knowing that *ea* is nonlocal parameter, Eq. (2) results in below field components for the smart nano-scale beam containing stain and electro-magnetic field:

$$(1 - (ea)^2 \nabla^2)\sigma_{xx} = \tilde{C}_{11}\varepsilon_{xx} - \tilde{e}_{31}E_z - \tilde{q}_{31}H_z \qquad (12)$$

$$(1 - (ea)^2 \nabla^2)D_x = +\tilde{s}_{11}E_x + \tilde{d}_{11}H_x \qquad (13)$$

$$(1 - (ea)^2 \nabla^2)D_z = \tilde{e}_{31}\varepsilon_{xx} + \tilde{s}_{33}E_z + \tilde{d}_{33}H_z \qquad (14)$$

$$(1 - (ea)^2 \nabla^2)B_x = +\tilde{d}_{11}E_x + \tilde{\chi}_{11}H_x \qquad (15)$$

$$(1 - (ea)^2 \nabla^2)B_z = \tilde{q}_{31}\varepsilon_{xx} + \tilde{d}_{33}E_z + \tilde{\chi}_{33}H_z \qquad (16)$$

Reduced forms of the constants C_{ij}, e_{ij} and q_{ij} can be found in the literature. Five governing equations for the curved smart nanobeam can be expressed as:

$$\frac{\partial N_{xx}}{\partial x} = 0 \qquad (17)$$

$$\frac{\partial^2 M_{xx}}{\partial x^2} + (N_{x0} + N_{xx})\left(\frac{\partial^2 w}{\partial x^2}\right) = q \qquad (18)$$

$$\int_{-h/2}^{h/2} \left(\cos(\xi z)\frac{\partial D_x}{\partial x} + \xi \sin(\xi z)D_z\right) dz = 0 \qquad (19)$$

$$\int_{-h/2}^{h/2} \left(\cos(\xi z)\frac{\partial B_x}{\partial x} + \xi \sin(\xi z)B_z\right) dz = 0 \qquad (20)$$

where $q = q_0$ is the transverse uniform mechanical load. Also, note that N_{ij} and M_{ij} (ij=xx) describe membrane forces and bending moments:

$$N_{xx} = \int_{-h/2}^{h/2}(\sigma_{xx})dz, \quad M_{xx} = \int_{-h/2}^{h/2} z(\sigma_{xx})dz \qquad (21)$$

Herein, this is supposed that the smart nano-sized beam is affected by outer electrical voltages and magnetic potentials. Accordingly, N_{x0} defines the in-plane loading owning to external electrical voltages V, magnetic potentials Ω and temperature ΔT is defined as:

$$N_{x0} = N^E + N^H + N^T, \quad N^E = -\int_{-\frac{h}{2}}^{\frac{h}{2}}\tilde{e}_{31}\frac{2V_E}{h}dz, \quad N^H = -\int_{-h/2}^{h/2}\tilde{q}_{31}\frac{2\Omega}{h}dz \qquad (22)$$

Based upon Hamilton's rule, it is feasible to express correlated edge conditions for MEE nano-scale beam based upon n_x as cosines of directions:

$$u = 0, or N_{xx}n_x = 0 \qquad (23)$$

$$w = 0, or n_x\left(\frac{\partial M_{xx}}{\partial x} - N_{x0}\frac{\partial w}{\partial x}\right) = 0 \qquad (24)$$

$$\frac{\partial w}{\partial x} = 0, or M_{xx}n_x = 0 \tag{25}$$

$$\phi = 0, \ or \int_{-h/2}^{h/2}(cos(\xi z)D_x n_x)dz = 0 \tag{26}$$

$$\gamma = 0, \ or \int_{-h/2}^{h/2}(cos(\xi z)B_x n_x)dz = 0 \tag{27}$$

Determining the integrals represented in Eq. (21) gives the below equations for smart nano-size beams in the context of nonlocal theory as:

$$(1 - (ea)^2\nabla^2)N_{xx} = A_{11}(\frac{\partial u}{\partial x} + \frac{1}{2}(\frac{\partial w}{\partial x})^2) - B_{11}\frac{\partial^2 w}{\partial x^2} + A_{31}^e\phi + A_{31}^m\gamma \tag{28}$$

$$(1 - (ea)^2\nabla^2)M_{xx} = B_{11}(\frac{\partial u}{\partial x} + \frac{1}{2}(\frac{\partial w}{\partial x})^2) - D_{11}\frac{\partial^2 w}{\partial x^2} + E_{31}^e\phi + E_{31}^m\gamma \tag{29}$$

$$\int_{-h/2}^{h/2}(1 - (ea)^2\nabla^2)D_x \, cos(\xi z)dz = + F_{11}^e\frac{\partial\phi}{\partial x} + F_{11}^m\frac{\partial\gamma}{\partial x} \tag{30}$$

$$\int_{-h/2}^{h/2}(1 - (ea)^2\nabla^2)D_z\xi \, sin(\xi z)dz = A_{31}^e(\frac{\partial u}{\partial x} + \frac{1}{2}(\frac{\partial w}{\partial x})^2) - E_{31}^e(\frac{\partial^2 w}{\partial x^2}) - F_{33}^e\phi - F_{33}^m\gamma \tag{31}$$

$$\int_{-h/2}^{h/2}(1 - (ea)^2\nabla^2)B_x \, cos(\xi z)dz = + F_{11}^m\frac{\partial\phi}{\partial x} + X_{11}^m\frac{\partial\gamma}{\partial x} \tag{32}$$

$$\int_{-h/2}^{h/2}(1 - (ea)^2\nabla^2)B_z\xi \, sin(\xi z)dz = A_{31}^m(\frac{\partial u}{\partial x} + \frac{1}{2}(\frac{\partial w}{\partial x})^2) - E_{31}^m(\frac{\partial^2 w}{\partial x^2}) - F_{33}^m\phi - X_{33}^m\gamma \tag{33}$$

so that

$$\{A_{11}, B_{11}, D_{11}\} = \int_{-h/2}^{h/2}\tilde{C}_{11}\{1, z, z^2\}dz, \tag{34}$$

$$\{A_{12}, B_{12}, D_{12}\} = \int_{-h/2}^{h/2}\tilde{C}_{12}\{1, z, z^2\}dz, \tag{35}$$

$$\{A_{66}, B_{66}, D_{66}\} = \int_{-h/2}^{h/2}\tilde{C}_{66}\{1, z, z^2\}dz, \tag{36}$$

$$\{A_{31}^e, E_{31}^e\} = \int_{-h/2}^{h/2}\tilde{e}_{31}\xi \, sin(\xi z)\{1, z\} \, dz \tag{37}$$

$$\{A_{31}^m, E_{31}^m\} = \int_{-h/2}^{h/2}\tilde{q}_{31}\xi \, sin(\xi z)\{1, z\} \, dz \tag{38}$$

$$\{F_{11}^e, F_{22}^e, F_{33}^e\} = \int_{-h/2}^{h/2} \{\tilde{s}_{11} \cos^2(\xi z), \tilde{s}_{22} \cos^2(\xi z), \tilde{s}_{33} \xi^2 \sin^2(\xi z)\} \, dz \tag{39}$$

$$\{F_{11}^m, F_{22}^m, F_{33}^m\} = \int_{-h/2}^{h/2} \{\tilde{d}_{11} \cos^2(\xi z), \tilde{d}_{22} \cos^2(\xi z), \tilde{d}_{33} \xi^2 \sin^2(\xi z)\} \, dz \tag{40}$$

$$\{X_{11}^m, X_{22}^m, X_{33}^m\} = \int_{-h/2}^{h/2} \{\tilde{\chi}_{11} \cos^2(\xi z), \tilde{\chi}_{22} \cos^2(\xi z), \tilde{\chi}_{33} \xi^2 \sin^2(\xi z)\} \, dz \tag{41}$$

The governing equations of thin nano-size beam based upon the displacement components and potential components might be determined with the insertion of Eqs. (28)-(33) into Eqs. (17)-(20) as:

$$A_{11}\left(\frac{\partial^2 u}{\partial x^2} + \frac{\partial^2 w}{\partial x^2}\frac{\partial w}{\partial x}\right) - B_{11}\frac{\partial^3 w}{\partial x^3} + A_{31}^e\frac{\partial \phi}{\partial x} + A_{31}^m\frac{\partial \gamma}{\partial x} = 0 \tag{42}$$

$$\begin{aligned}
&B_{11}\left(\frac{\partial^3 u}{\partial x^3} + \frac{\partial^3 w}{\partial x^3}\frac{\partial w}{\partial x} + \frac{\partial^2 w}{\partial x^2}\frac{\partial^2 w}{\partial x^2}\right) - D_{11}\frac{\partial^4 w}{\partial x^4} + E_{31}^e\left(\frac{\partial^2 \phi}{\partial x^2}\right) + E_{31}^m\left(\frac{\partial^2 \gamma}{\partial x^2}\right) \\
&+\frac{1}{R}\left[A_{11}\left(\frac{\partial u}{\partial x} + \frac{1}{2}\left(\frac{\partial w}{\partial x}\right)^2\right) - B_{11}\frac{\partial^2 w}{\partial x^2} + A_{31}^e\phi + A_{31}^m\gamma\right] \\
&+(1 - (ea)^2\nabla^2)\left(A_{11}\left(\frac{\partial u}{\partial x} + \frac{1}{2}\left(\frac{\partial w}{\partial x}\right)^2\right) - B_{11}\frac{\partial^2 w}{\partial x^2} + A_{31}^e\phi + A_{31}^m\gamma\right)\left(\frac{\partial^2 w}{\partial x^2}\right) \\
&+(1 - (ea)^2\nabla^2)\left[-(N^E + N^H + N^T)\left(\frac{\partial^2 w}{\partial x^2} + \frac{\partial^2 w}{\partial y^2}\right)\right] = q
\end{aligned} \tag{43}$$

$$+F_{11}^e\frac{\partial^2 \phi}{\partial x^2} + F_{11}^m\frac{\partial^2 \gamma}{\partial x^2} + A_{31}^e\left(\frac{\partial u}{\partial x} + \frac{1}{2}\left(\frac{\partial w}{\partial x}\right)^2\right) - E_{31}^e\left(\frac{\partial^2 w}{\partial x^2}\right) - F_{33}^e\phi - F_{33}^m\gamma = 0 \tag{44}$$

$$+F_{11}^m\frac{\partial^2 \phi}{\partial x^2} + X_{11}^m\frac{\partial^2 \gamma}{\partial x^2} + A_{31}^m\left(\frac{\partial u}{\partial x} + \frac{1}{2}\left(\frac{\partial w}{\partial x}\right)^2\right) - E_{31}^m\left(\frac{\partial^2 w}{\partial x^2}\right) - F_{33}^m\phi - X_{33}^m\gamma = 0 \tag{45}$$

5. Solution by differential quadrature method (DQM)

In the present chapter, differential quadrature method (DQM) has been utilized for solving the governing equations for the smart nanobeam. According to DQM, at an assumed grid point (x_i, y_j) the derivatives for function F are supposed as weighted linear summation of all functional values within the computation domains as:

$$\frac{d^n F}{dx^n}\Big|_{x=x_i} = \sum_{j=1}^{N} c_{ij}^{(n)} F(x_j) \tag{46}$$

where

$$C_{ij}^{(1)} = \frac{\pi(x_i)}{(x_i - x_j)\,\pi(x_j)} \qquad i,j = 1,2,\dots,N, \qquad i \neq j \tag{47}$$

in which $\pi(x_i)$ is defined by

$$\pi(x_i) = \prod_{j=1}^{N}(x_i - x_j), \quad i \neq j \tag{48}$$

and when $i = j$

$$C_{ij}^{(1)} = c_{ii}^{(1)} = -\sum_{k=1}^{N} C_{ik}^{(1)}, \quad i = 1,2,\dots,N, \quad i \neq k, \quad i = j \tag{49}$$

Then, weighting coefficients for high orders derivatives may be expressed by:

$$C_{ij}^{(2)} = \sum_{k=1}^{N} C_{ik}^{(1)} C_{kj}^{(1)}, \ C_{ij}^{(3)} = \sum_{k=1}^{N} C_{ik}^{(1)} C_{kj}^{(2)} = \sum_{k=1}^{N} C_{ik}^{(2)} C_{kj}^{(1)}$$

$$C_{ij}^{(4)} = \sum_{k=1}^{N} C_{ik}^{(1)} C_{kj}^{(3)} = \sum_{k=1}^{N} C_{ik}^{(3)} C_{kj}^{(1)} \qquad i,j = 1,2,\dots,N. \ , \tag{50}$$

$$C_{ij}^{(5)} = \sum_{k=1}^{N} C_{ik}^{(1)} C_{kj}^{(4)} = \sum_{k=1}^{N} C_{ik}^{(4)} C_{kj}^{(1)}, \ C_{ij}^{(6)} = \sum_{k=1}^{N} C_{ik}^{(1)} C_{kj}^{(5)} = \sum_{k=1}^{N} C_{ik}^{(5)} C_{kj}^{(1)}$$

According to presented approach, the dispersions of grid points based upon Gauss-Chebyshev-Lobatto assumption are expressed as:

$$x_i = \frac{L}{2}\left[1 - \cos\left(\frac{i-1}{N-1}\pi\right)\right] \quad i = 1,2,\dots,N, \tag{51}$$

Next, the displacement components may be re-written by

$$\{u,w,\phi,\gamma\}(x) = \{U,W,\Phi,\Upsilon\}(x)e^{i\omega_n t} \tag{52}$$

where $\{U,W,\Phi,\Upsilon\}$ are the amplitudes. Then, it is possible to express obtained boundary conditions as:

$$\phi = \gamma = w = 0, \qquad \frac{\partial^2 w}{\partial x^2} = 0 \tag{53}$$

Now, one can express the modified weighting coefficients for all edges simply-supported as:

$$\bar{C}_{1,j}^{(2)} = \bar{C}_{N,j}^{(2)} = 0, \quad i = 1,2,\dots,M, \ \bar{C}_{i,1}^{(2)} = \bar{C}_{1,M}^{(2)} = 0, \quad i = 1,2,\dots,N. \tag{54}$$

and

$$\bar{C}_{ij}^{(3)} = \sum_{k=1}^{N} C_{ik}^{(1)} \bar{C}_{kj}^{(2)} \qquad\qquad \bar{C}_{ij}^{(4)} = \sum_{k=1}^{N} C_{ik}^{(1)} \bar{C}_{kj}^{(3)} \tag{55}$$

Considering DQ solution and including displacements represented in Eq. (52) into Eqs. (42)-(45) yields the following ordinary nonlinear governing equations as:

$$k_{11}U + k_{21}W + n_1 W^2 + k_{31}\Phi + k_{41}\Upsilon = 0 \tag{56}$$

$$k_{12}U + k_{22}W + n_3 W^2 + n_4 W^3 + n_5 UW + k_{32}\Phi + k_{42}\Upsilon + n_9 \Phi W + n_{10}\Upsilon W = Q \tag{57}$$

$$k_{13}U + k_{23}W + n_7 W^2 + k_{33}\Phi + k_{43}\Upsilon = 0 \tag{58}$$

$$k_{14}U + k_{24}W + n_8 W^2 + k_{34}\Phi + k_{44}\Upsilon = 0 \tag{59}$$

It must be expressed that n_i and k_{ij} display the components of stiffness matrix respectively in

non-linear and linear forms. Owning to this deduction that there are 4 governing equations which are coupled together, providing the closed-form of non-linear bending load as a function of shell deflection (W) is too hard. Thus, by simultaneous solve of Eqs. (56), (58) and (59), it is feasible to calculate displacements (U, Φ, Υ) as functions of beam deflections (W). Next, determined amplitudes $(\widehat{U}, \widehat{\Phi}, \widehat{\Upsilon})$ have been placed in Eq. (57) in order to determine only one nonlinear equation for the smart beam as:

$$k_{12}\widehat{U} + k_{22}W + n_3 W^2 + n_4 W^3 + n_5 \widehat{U}W + k_{32}\widehat{\Phi} + k_{42}\widehat{\Upsilon} + n_9 \widehat{\Phi}W + n_{10}\widehat{\Upsilon}W = Q \tag{60}$$

By simplifying the obtained equation, the above equation may be obtained as:

$$\frac{K_1}{M}\widetilde{W} + \frac{K_2}{M}\widetilde{W}|\widetilde{W}| + \frac{K_3}{M}\widetilde{W}^3 = Q \tag{61}$$

It must be pointed out that K_1, K_2 and K_3 have complex forms and expressing their closed forms is very difficult. Solving the Eq. (61) will give the load-deflection curves of the nanobeam. The unit of the load in nN. To present obtained results, non-dimension nonlocal parameter can be defined by:

$$\mu = \frac{ea}{a} \tag{62}$$

6. Results and discussions

In this chapter, impacts of different factors such as magneto-electrical field, nonlocality, temperature and material compositions on nonlinear bending curves of smart piezo-magnetic nanobeams have been examined. The thickness of nano-sized beam has been chosen to be $h = 1$ nm.
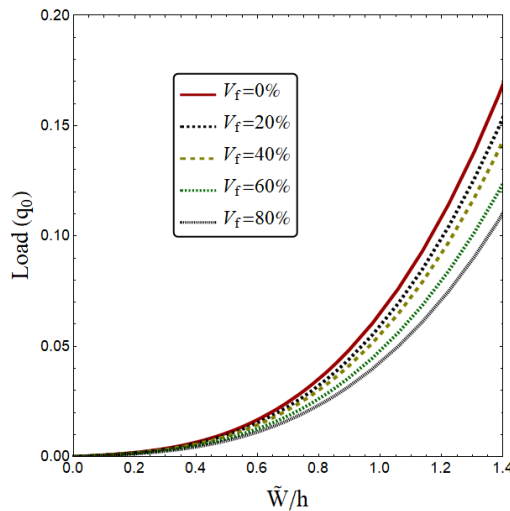

Fig. 2 Load-deflection curves of the smart nanoscale beam with varying piezoelectric phase percentage ($L/h = 20$, $V_E = 0$, $\mu = 0.2$)
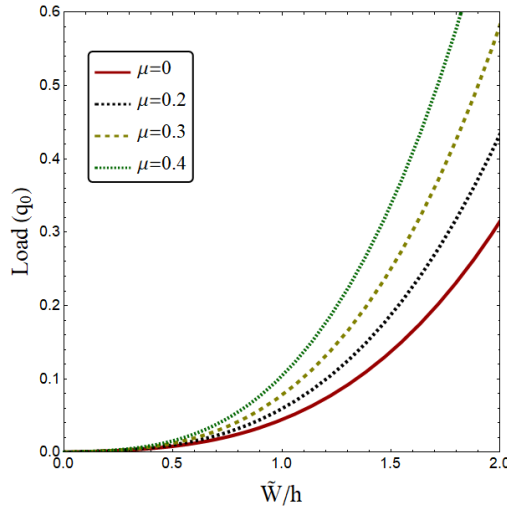
Fig. 3 Load-deflection curves of the smart nanoscale beam with varying nonlocal parameter (L/h = 20, V_f = 20%)
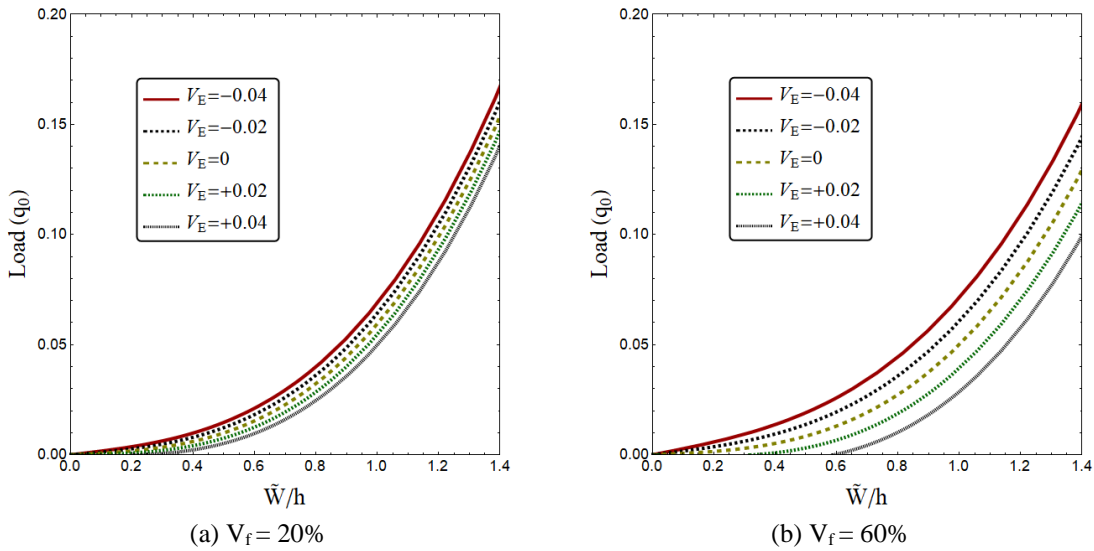

(a) $V_f = 20\%$ (b) $V_f = 60\%$

Fig. 4 Load-deflection curves of the smart nanoscale beam with varying electrical voltage (L/h = 20, μ = 0.2)

Fig. 2 illustrates the variation of bending load of smart nanscale beam against non-dimension deflection, for diverse piezoelectric phase percentages (V_f). The nonlocality scale factor is set to be μ = 0.2. Genrally speaking, the load magnitude increases with the increase of beam deflection. Also, increasing in the value of V_f is corresponding to higher portion of piezoelectric phase and lower portion of magnetic phase. Actually, increase of V_f leads to lower elastic modolus of the two-phase composite material as indicated in Table 1. This means that the load value (q_0) is reducing with increasing in piezoelectric phase percentage. Accordingly, the load bearing capacity of the smart nanobeam has been decreased.
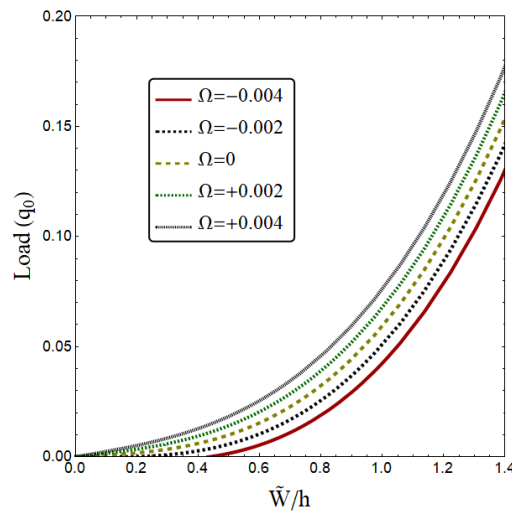
Fig. 5 Load-deflection curves of the smart nanoscale beam with varying magnetic field intensity (L/h = 20, V_f = 20%, μ = 0.2)
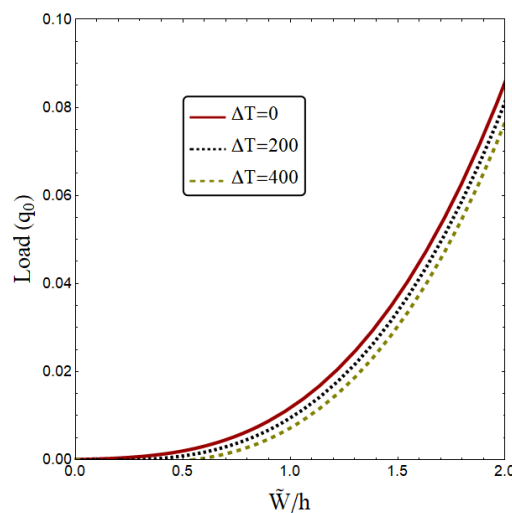

Fig. 6 Load-deflection curves of the smart nanoscale beam with varying temperature (L/h = 30, V_f = 20%, μ = 0.2)

Load-deflection curves of the smart nanoscale beam with varying nonlocal parameter have been plotted in Fig. 3 assuming V_f = 20%. The nano-dimension beam length is selected to be L=20h. It can be concluded that the bending load values of nonlocal smart nano-size beams may be higher than that of local macro-sized beam. Also, the beam deflection is increasing with the growth of nonlocality factor due to the reduction in nanobeam stiffness. Therefore, static behavior of a nano-size beam is dependent on the value of nonlocality parameter.

In Fig. 4, changing of bending load of intellgent nanobeam versus non-dimension deflection is illustrated for diverse electrical voltages (V_E) and piezoelectric phase percentage (V_f = 20%, 60%). It can be inferred that load-deflection curves of nano-dimension smart beams are notably

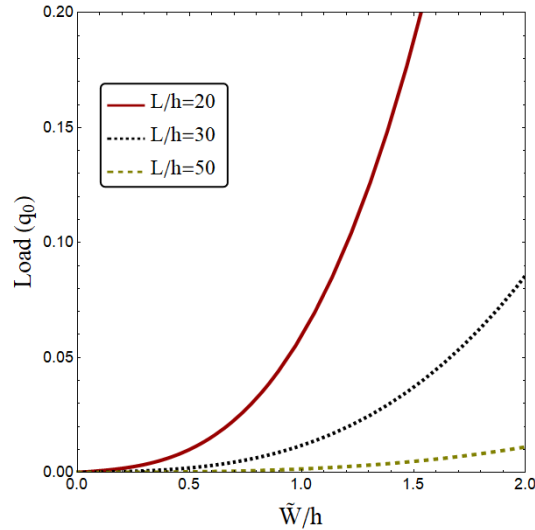Fig. 7 Load-deflection curves of the smart nanoscale beam with varying length-to-thickness ratio (V_f = 20%, μ = 0.2)

affected by the value and sign of electrical voltage. One can observe that negative electrical voltages provide higher load-deflection curves than positive voltages. The difference in such a behavior is due to the exertion of tensile forces by negative voltages and compressive forces by the positive voltages. Also, comparing the provided curves by assuming V_f = 20% and 60%, it can be deduced that the load-deflection curves are more dependent on the electrical voltages at V_f = 60%. This is related to the inclusion of more piezoelectric phase in the composite material.

Fig. 5 demonstrates the influences of magnetic field intensities on load-deflection curves of the smart nano-scaled beams when V_f = 20%, μ = 0.2. It may be especified that negative values for magnetic intensity give lower load-deflection curves than positive magnetic intensity. Actually, the applied negative/positive magnetic intensities might produce the in-plane compressive/tensile loads. Whereas, electrical fields showed an opposite influence. As a conclusion, it is clear that the deflection curves can be controlled via applying a suitbale value of electrical voltage or magnetic intensity.

7. Conclusions

Bending characteristics of a piezo-magnetic nanobeam with uniform thickness were reported in the present article. The complete formulation and solution for the problem based on thin beam model was presented. It was clarified that the stability behaviors of the nano-size smart beam are affected by piezoelectric phase percentage. There was more change in load-deflection curves versus applied voltage when the piezoelectric volume fraction was increased. Also, applying positive or negative magnetic potentials led to increasing or reducing the stability load. Another observation was that size effects due to nonlocality changed significantly the load-deflection curves of piezo-magnetic nano-sized beam. The bemding deflection could be controlled via applying a suitbale value of electrical voltage or magnetic intensity.

Acknowledgement

References

Abderezak, R., Daouadji, T.H. and Rabia, B. (2021), "Modeling and analysis of the imperfect FGM-damaged RC hybrid beams", *Adv. Comput. Des.*, **6**(2), 117-133. https://doi.org/10.12989/acd.2021.6.2.117.

Abdullah, W.N., Khalaf, B.S., Ahmed, R.A., Fenjan, R.M. and Faleh, N.M. (2021), "Thermal effects on dynamic response of GOP-Reinforced beams under blast load", *Adv. Concr. Constr.*, **12**(3), 167-174. https://doi.org/10.12989/acc.2021.12.3.167.

Abdulrazzaq, M.A., Muhammad, A.K., Kadhim, Z.D. and Faleh, N.M. (2020), "Vibration analysis of nonlocal strain gradient porous FG composite plates coupled by visco-elastic foundation based on DQM", *Coupled Syst. Mech.*, **9**(3), 201-217. https://doi.org/10.12989/csm.2020.9.3.201.

Ahmed, R.A., Fenjan, R.M. and Faleh, N.M. (2019), "Analyzing post-buckling behavior of continuously graded FG nanobeams with geometrical imperfections," *Geomech. Eng.*, **17**(2), 175-180. https://doi.org/10.12989/gae.2019.17.2.175.

Ahmed, R.A., Fenjan, R.M., Hamad, L.B. and Faleh, N.M. (2020), "A review of effects of partial dynamic loading on dynamic response of nonlocal functionally graded material beams", *Adv. Mater. Res.*, **9**(1), 33-48. https://doi.org/10.12989/amr.2020.9.1.033.

Ahmed, R.A., Al-Toki, M.H., Faleh, N.M. and Fenjan, R.M. (2021), "Nonlinear stability of higher-order porous metal foam curved panels with stiffeners", *Transp. Porous Med.*, 1-16. https://doi.org/10.1007/s11242-021-01691-2.

Akbaş, Ş.D. (2016), "Forced vibration analysis of viscoelastic nanobeams embedded in an elastic medium", *Smart Struct. Syst.*, **18**(6), 1125-1143. http://doi.org/10.12989/sss.2016.18.6.1125.

Al-Maliki, A.F., Faleh, N.M. and Alasadi, A.A. (2019), "Finite element formulation and vibration of nonlocal refined metal foam beams with symmetric and non-symmetric porosities", *Struct. Monit. Maint.*, **6**(2), 147-159. https:// doi.org/10.12989/smm.2019.6.2.147.

Al-Maliki, A.F., Ahmed, R.A., Moustafa, N.M. and Faleh, N.M. (2020), "Finite element based modeling and thermal dynamic analysis of functionally graded graphene reinforced beams", *Adv. Comput. Des.*, **5**(2), 177-193. https://doi.org/10.12989/acd.2020.5.2.177.

Eringen, A.C. (1972), "Linear theory of nonlocal elasticity and dispersion of plane waves", *Int. J. Eng. Sci.*, **10**(5), 425-435. https://doi.org/10.1016/0020-7225(72)90050-X.

Fenjan, R.M., Ahmed, R.A., Alasadi, A.A. and Faleh, N.M. (2019), "Nonlocal strain gradient thermal vibration analysis of double-coupled metal foam plate system with uniform and non-uniform porosities", *Coupled Syst. Mech.*, **8**(3), 247-257. https://doi.org/10.12989/csm.2019.8.3.247.

Fenjan, R.M., Hamad, L.B. and Faleh, N.M. (2020a), "Mechanical-hygro-thermal vibrations of functionally graded porous plates with nonlocal and strain gradient effects", *Adv. Aircr. Spacecr. Sci.*, **7**(2), 169-186. https://doi.org/10.12989/aas.2020.7.2.169.

Fenjan, R.M., Ahmed, R.A., Hamad, L.B. and Faleh, N.M. (2020b), "A review of numerical approach for dynamic response of strain gradient metal foam shells under constant velocity moving loads", *Adv. Comput. Des.*, **5**(4), 349-362. https://doi.org/10.12989/acd.2020.5.4.349.

Guo, J., Chen, J. and Pan, E. (2016), "Static deformation of anisotropic layered magnetoelectroelastic plates based on modified couple-stress theory", *Compos. Part B Eng.*, **107**, 84-96. https://doi.org/10.1016/j.compositesb.2016.09.044.

Hamad, L.B., Khalaf, B.S. and Faleh, N.M. (2019), "Analysis of static and dynamic characteristics of strain

gradient shell structures made of porous nano-crystalline materials", *Adv. Mater. Res.*, **8**(3), 179-96.
https://doi.org/10.12989/amr.2019.8.3.179.

Heydari, A. (2020), "Buckling analysis of noncontinuous linear and quadratic axially graded Euler beam subjected to axial span-load in the presence of shear layer", *Adv. Comput. Des.*, **5**(4), 397-416.
https://doi.org/10.12989/acd.2020.5.4.397.

Jiang, L., Wang, Y., Wang, X., Ning, F., Wen, S., Zhou, Y. and Zhou, F.L. (2021), "Electrohydrodynamic printing of a dielectric elastomer actuator and its application in tunable lenses", *Compos. Part A Appl. S.*, **147**, 106461. https://doi.org/10.1016/j.compositesa.2021.106461.

Ke, L.L., Wang, Y.S., Yang, J. and Kitipornchai, S. (2014), "The size-dependent vibration of embedded magneto-electro-elastic cylindrical nanoshells", *Smart Mater. Struct.*, **23**(12), 125036.
https://doi.org/10.1088/0964-1726/23/12/125036.

Kumaravel, A., Ganesan, N. and Sethuraman, R. (2007), "Buckling and vibration analysis of layered and multiphase magneto-electro-elastic beam under thermal environment", *Multidiscip. Model. Mater. Struct.*, **3**(4), 461-476. https://doi.org/10.1163/157361107782106401.

Li, Y. and Shi, Z. (2009), "Free vibration of a functionally graded piezoelectric beam via state-space based differential quadrature", *Compos. Struct.*, **87**(3), 257-264.
https://doi.org/10.1016/j.compstruct.2008.01.012.

Liu, H., Liu, H. and Yang, J. (2018), "Vibration of FG magneto-electro-viscoelastic porous nanobeams on visco-Pasternak foundation", *Compos. Part B Eng.*, **155**, 244-256.
https://doi.org/10.1016/j.compositesb.2018.08.042.

Muhammad, A.K., Hamad, L.B., Fenjan, R.M. and Faleh, N.M. (2019), "Analyzing large-amplitude vibration of nonlocal beams made of different piezo-electric materials in thermal environment", *Adv. Mater. Res.*, **8**(3), 237-257. https://doi.org/10.12989/amr.2019.8.3.237.

Pan, E. and Han, F. (2005), "Exact solution for functionally graded and layered magneto-electro-elastic plates", *Int. J. Eng. Sci.*, **43**(3-4), 321-339. https://doi.org/10.1016/j.ijengsci.2004.09.006.

Polatov, A.M., Khaldjigitov, A.A. and Ikramov, A.M. (2020), "Algorithm of solving the problem of small elastoplastic deformation of fiber composites by FEM", *Adv. Comput. Des.*, **5**(3), 305-321.
https://doi.org/10.12989/acd.2020.5.3.305.

Raheef, K.M., Ahmed, R.A., Nayeeif, A.A., Fenjan, R.M. and Faleh, N.M. (2021), "Analyzing dynamic response of nonlocal strain gradient porous beams under moving load and thermal environment", *Geomech. Eng.*, **26**(1), 89-99. https://doi.org/10.12989/gae.2021.26.1.089.

Singh, A. and Kumari, P. (2020), "Analytical free vibration solution for angle-ply piezolaminated plate under cylindrical bending: A piezo-elasticity approach", *Adv. Comput. Des.*, **5**(1), 55-89.
https://doi.org/10.12989/acd.2020.5.1.055.

Thai, H.T. and Vo, T.P. (2012), "A nonlocal sinusoidal shear deformation beam theory with application to bending, buckling, and vibration of nanobeams", *Int. J. Eng. Sci.*, **54**, 58-66.
https://doi.org/10.1016/j.ijengsci.2012.01.009.

Zhou, H., Xu, C., Lu, C., Jiang, X., Zhang, Z., Wang, J. and Wang, L. (2021), "Investigation of transient magnetoelectric response of magnetostrictive/piezoelectric composite applicable for lightning current sensing", *Sensors Actuat. A Phys.*, **329**, 112789. https://doi.org/10.1016/j.sna.2021.112789.

CC